SSRG International Journal of Electrical and Electronics Engineering
ISSN: 2348-8379 / https://doi.org/10.14445/23488379/IJEEE-V10I2P112

Volume 10 Issue 2, 122-131, February 2023

Original Article

A Novel 5G Magneto-Electric Dipole Antenna with a Unique and Simplified Co-Axial Feeding Method for Mitigation of Fabrication Imperfections in Volumetric Antenna Designs

Pranav Bhatt[1], Komal R. Borisagar[2], Nirali Kotak[3]

[1]*Cyber Security and Digital Forensics, National Forensic Sciences University, Gujarat, India.*
[2]*Graduate School of Engineering and Technology, Gujarat Technological University, Gujarat, India.*
[3]*Electronics and Communication Department, L. D. College of Engineering, Gujarat Technological University, Gujarat, India.*

[1]*Corresponding Author: pranavm153@gmail.com*

Received: 09 January 2023 Revised: 08 February 2023 Accepted: 18 February 2023 Published: 28 February 2023

Abstract *- A novel low-profile coaxial-fed Magneto-electric dipole antenna for fifth-generation mobile technology is presented here. The antenna contains a simplified and robust feeding mechanism. A new design concept for the mitigation of fabrication errors is hypothesized and proved here. The final proposed antenna has an impedance bandwidth of 11.63 GHz (23.47-35.10 GHz), covering both the n257 and n258 bands. A stable and approximately identical E- and H-plane radiation pattern with a maximum total gain of 6.9 dB is achieved here.*

Keywords *- Co-axial feeding, Fabrication imperfection mitigation, ME dipole, 5G antenna, 5G base station antenna.*

1. Introduction

The exponential growth of wireless Internet-of-things devices and smartphones are the main drivers for researching and developing a very high data rate communication infrastructure. [1-3] There has been a consistent rise in internet users, reaching more than 90% in many economically developed countries. [4] The fifth-generation mobile technology (5G) contains the potential to fulfill this enormous data traffic. [5, 6] The frequency bands for 5G communication is divided into two frequency ranges, Frequency Range 1 (410 MHz-7125 MHz) and Frequency Range 2 (24.25 GHz – 52.6 GHz). [32] The Frequency Range 2 (FR2) is usually referred to as the 5G millimeter wave (mmWave) spectrum, and nowadays, it has grabbed huge attention from the research community. [8-10] To this date, several mmWave antennas have been reported in the literature.

In [11], researchers have co-designed conformal 4G long-term evolution and mmWave antenna having operating bands 2.5-2.53 GHz and 27-29 GHz, respectively. In, [12] the authors have designed a metal plate-backed bow-tie-shaped printed monopole antenna with a wideband response in millimeter wave range and out-of-the-band rejection capability. The antenna provided an acceptable reflection coefficient over the 22.2-28.9 GHz range with a gain varying between 0.8 to 6.6 dBi.

In [29], the authors have designed a thin substrate Magneto-Electric (ME) dipole antenna providing a reflection coefficient below 10 dB over the range 26.5-31 GHz with a gain above 5.5 dBi over the entire operating range. In [14], the researchers have designed a miniaturized dual-polarized wideband ME dipole antenna array that covers the entire Ka-band with an operating range from 26 GHz to 42 GHz.

This paper proposes a simple low-profile co-axial fed ME dipole antenna operating in the millimeter wave range, specifically covering n257 (26.50-29.50 GHz) and n258 (24.25-27.50 GHz) band, sometimes also referred to as LMDS and K-band, respectively. The ME dipole is selected for its advantages, like wide impedance bandwidth, stable gain over operating frequencies, low cross-polarization, and low back radiation levels.[15,16] The proposed design dimensions are adjusted considering the ease of design and the performance accuracy. The antenna structure positioning imperfections are also considered here in this paper.

2. Antenna Design

2.1. Luk and Wong ME Dipole Design

The original research of Luk and Wong on the Magneto-electric dipole antenna is used as a base for designing the proposed antenna.[30] The antenna proposed by Luk and Wong is shown in Figure 1. It contains three parts, vertical quarter-wave shorted patches as a magnetic dipole, a horizontal patch as an electric dipole, and a Γ-shaped feeding structure. Here in this paper, initially, a basic structure is designed using the imperial equations given by Luk and Wong, and after that, design optimization is performed. The design equations for the dimensions of the Magneto-electric dipole antenna are as follows.[30]

$$L = H = 0.25\lambda_0 \quad (1)$$

$$W = 0.50\lambda_0 \quad (2)$$

$$S = 0.14\lambda_0 \quad (3)$$

$$G = 1.33\lambda_0 \quad (4)$$

$$a = 0.08\lambda_0 \quad (5)$$

$$b = 0.18\lambda_0 \quad (6)$$

$$f = 0.04\lambda_0 \quad (7)$$

The center frequency for the n258 band is 25.875 GHz, so the corresponding wavelength λ_0 is 11.586 mm. So, from the Equation (1-7), the corresponding value of L for the λ_0 is 2.897 mm, W is 5.793 mm, S is 1.622 mm, H is 2.897 mm, G is 15.409 mm, a is 0.927 mm, b is 2.085 mm, and f is 0.463 mm. To avoid any design errors, the dimensions have three decimal places because, in the millimeter wave range, the minor variation in the dimension causes significant changes in results. The problem with the ME dipole design shown in Figure 1 is its Γ-shaped feed because it increases design complexity.[18] At the frequency of interest, a minor dimensional change in any portion of the feed results in deterioration of results like poor matching.

2.2. Coaxial-Fed Elementary ME Dipole Design

An alternative approach to removing the vertical plates and feed is to use a co-axial cable, the inner conductor of the co-axial cable is used to feed one of the horizontal plates, and the grounded outer conductor is connected to another plate. The vertical plates creating a magnetic dipole are also sometimes called a cavity.[19] So the initial design without a cavity is shown in Figure 2. The design dimensions are kept the same as the previously calculated ones using the empirical equations.

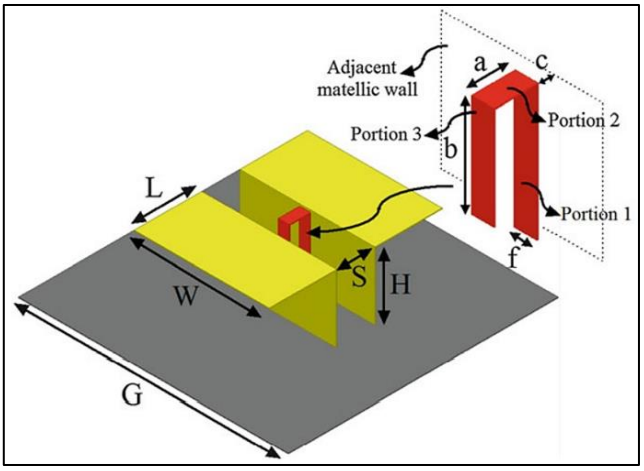

Fig. 1 Magneto-electric dipole antenna proposed by Luk and Wong [8]

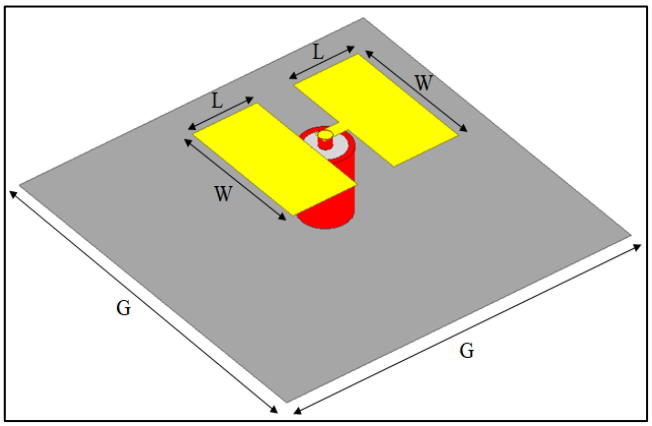

Fig. 2 Coaxial-fed magneto-electric dipole antenna

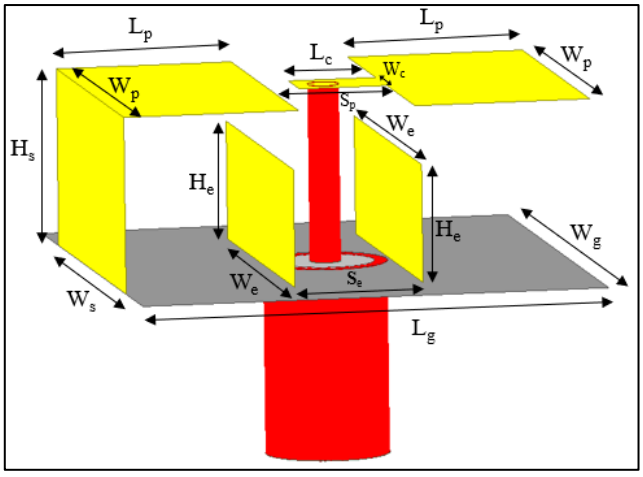

Fig. 3 Proposed magneto-electric antenna design

An additional small plate having the width same as that of the diameter of the inner conductor of the co-axial cable is used to hold the horizontal plate spacing symmetry with respect to the co-axial cable because, at millimeter wave, the antenna dimensions and the co-axial cable dimensions start to resemble one another. At a much lower frequency, the effect

of imperfection in the symmetry is in all respect negligible. By appropriately choosing the distance between the horizontal plates and the outer conductor of the co-axial cable, the antenna shown in Figure 2 can be simulated to give desired results. However, the issues are with the fabrication of the antenna. [20] It is utterly impossible to physically fabricate an antenna having fractional dimensions in millimeters with one decimal point, let alone two or three decimal points. The other issues are arrangement accuracy of co-axial feeding because unlike simple co-axial feeding, where the co-axial cable is connected at the bottom of the ground plane using the connector and the connector pin is used to feed the patch, here the distance between the horizontal plate and the outer conductor of the co-axial cable is less than the distance between the horizontal plate and the ground plane, so basically the outer conductor also crosses the ground plane causing the possibility of matching imperfection. In addition, the substrate is not used to improve the radiation efficiency, which creates concern about sustaining horizontal plates precisely parallel to the ground plane.[21, 22] The proposed solution is to realize an entire design with all integer dimensions to the extent possible.

2.3. Proposed Antenna Geometry

The proposed antenna shown in Figure 3 resolves all of the described issues. The antenna designing started with both patches having a size of 3 mm x 6 mm, considering it to be the respective closest integer value to the previously calculated dimensions using the empirical design equations.

The co-axial cable is positioned at the geometric center of the ground plane. At the geometric center of design in Figure 2, all the design segments are in closer proximity which increases the fabrication complexity considering the physical dimensions of the proposed antenna, shown in Table 1. To avoid this, a shorting plate with a 6 mm width and a 3 mm height is connected to the far end of the patch, as shown in Figure 3. The shorting plate is used instead of the shorting post considering its effectiveness in holding the patch precisely parallel to the ground plane due to the width of its edge (width).[27,28,31] A novel technique of adding two symmetrical plates with respect to the center conductor of the co-axial cable is proposed here to solve the inner-outer conductor separation accuracy and placement issue, as shown in Figure 3. These plates are named enhancement plates. The parametric study is performed to find the optimum height for the enhancement plates and the spacing between them. Figure 4 shows the parametric analysis for the height of the enhancement plates (H_e), and Figure 5 shows the parametric analysis for the spacing between the enhancement plates (S_e). The optimum values for those turned out to be 2 mm and 2.1 mm, respectively. Considering the ease of fabrication, all the parametric analyses will consider only integer values except for a single variation of S_e, which is 2.1 mm because of the value of the outer diameter of the co-axial cable used in the proposed fabricated antenna.

Table 1. Physical dimensions of the proposed antenna

Parameter	Value
Length of patches (L_p)	3 mm
Width of patches (W_p)	6 mm
Height of shorting plate (H_s)	3 mm
Width of shorting plate (W_s)	6 mm
Height of enhancement plates (H_e)	2 mm
Width of enhancement plates (W_e)	6 mm
Length of connecting plate (L_c)	1.5 mm
Width of connecting plate (W_c)	1 mm
Spacing between the patches (S_p)	2 mm
Spacing between the enhancement plates (S_e)	2.1 mm
Length of the ground plane (L_g)	8 mm
Width of the ground plane (W_g)	8 mm

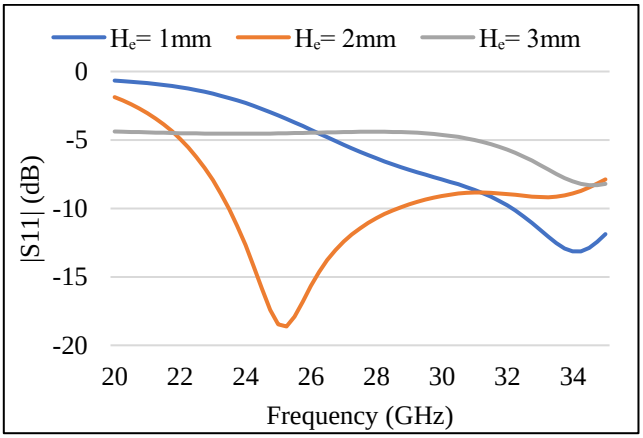

Fig. 4 Parametric analysis for the height of the enhancement plates

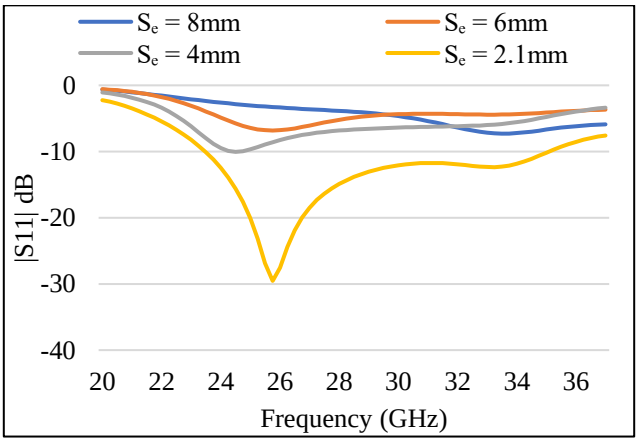

Fig. 5 Parametric analysis for spacing between the enhancement plates

Furthermore, to reduce the antenna's physical profile, the parametric analysis for the optimum size of the ground plane is performed, as shown in Figure 6, and its size turns out to be 8 mm x 8 mm. All values considered in the parametric studies range between the values found using empirical design equations and the respective minimum or maximum possible value for the selected parameter considering the values of the previously optimized parameter.

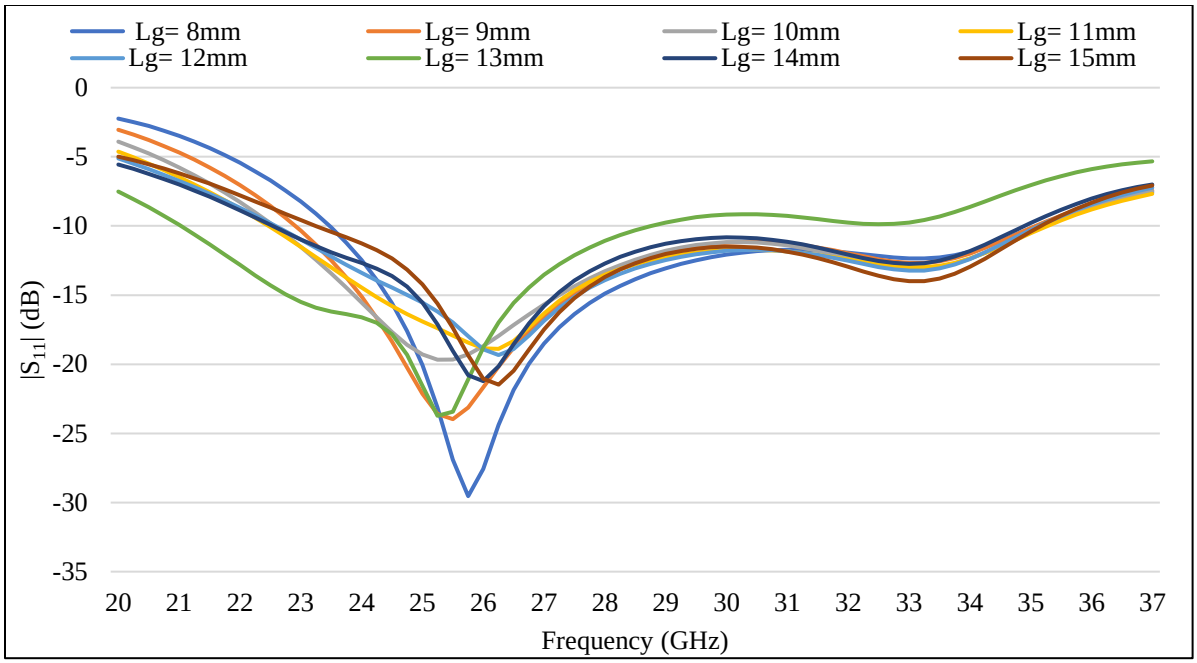

Fig. 6 Parametric analysis for the size of the ground plane

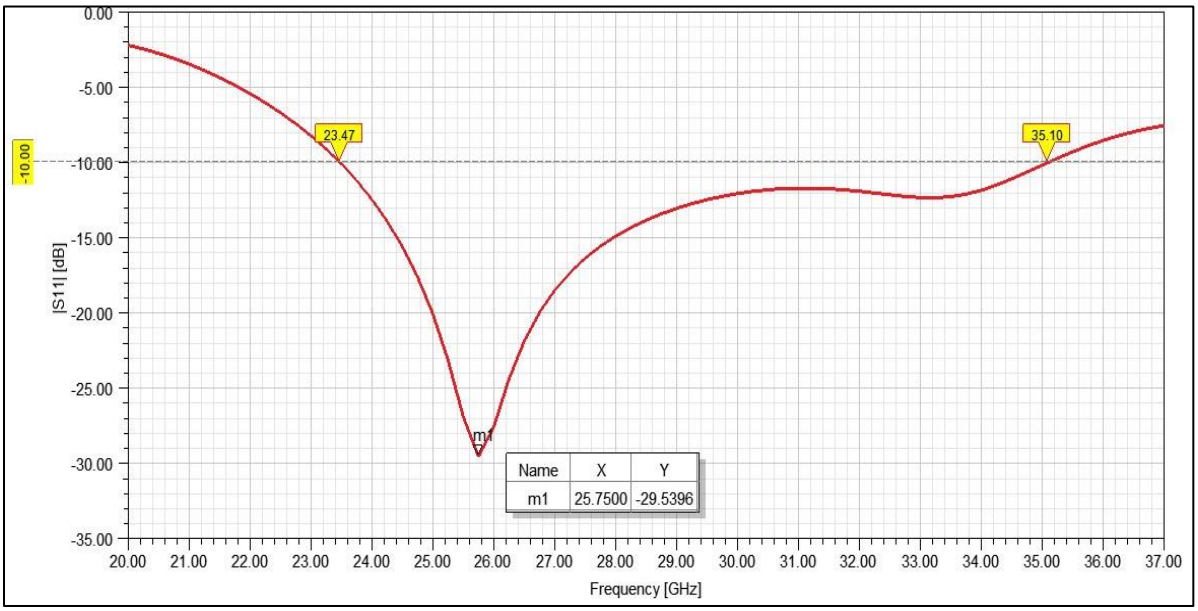

Fig. 7 Reflection coefficient curve of the proposed antenna

3. Results and Discussion

ANSYS Electronics Desktop 2020 R2 designs, simulates and optimizes the proposed antenna. The performance of the proposed antenna is evaluated with the help of the reflection coefficient curve, voltage standing wave ratio (VSWR), smith chart, and radiation patterns. The fabrication defects like enhancement plates' location errors and patch angular positioning errors are also considered here. The mitigation technique for that is also proposed here.

3.1. Reflection Coefficient Curve, VSWR and Smith Chart

It can be easily observed in Figure 7 that the proposed antenna covers both the n257 and n258 bands entirely. Also, both Figure 7 and Figure 8 show that the proposed antenna has an impedance bandwidth of 11.63 GHz (23.47-35.10 GHz), and it resonates at 25.75 GHz, attaining a return loss value as good as -30 dB. The smith chart in Figure 9 shows that matching is reasonably good over both bands.

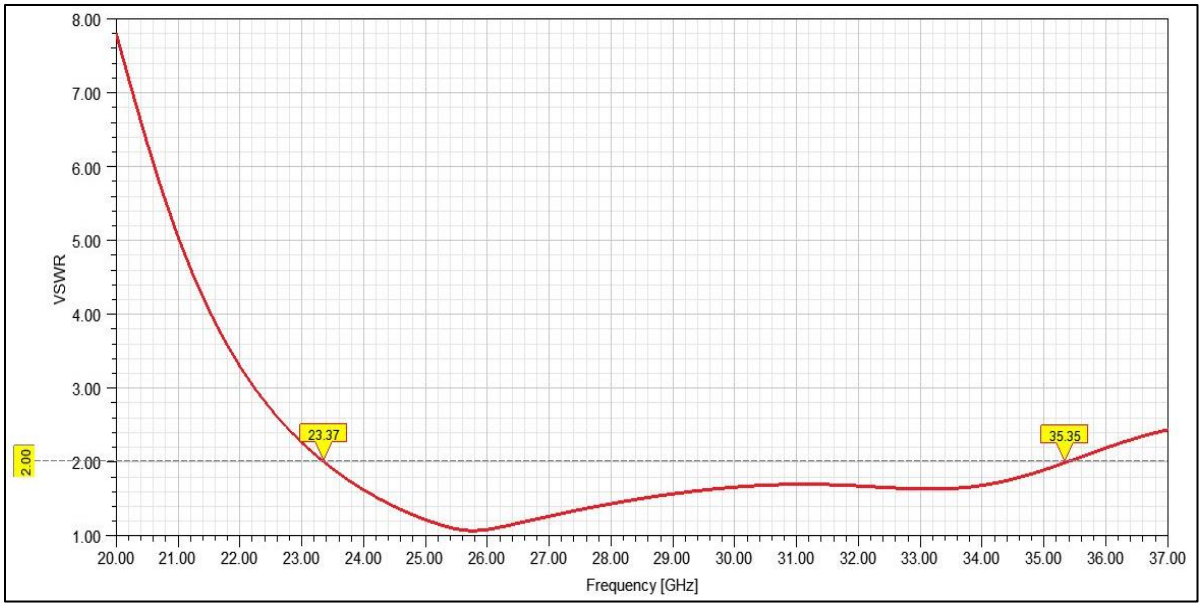

Fig. 8 VSWR vs. frequency plot for the proposed antenna

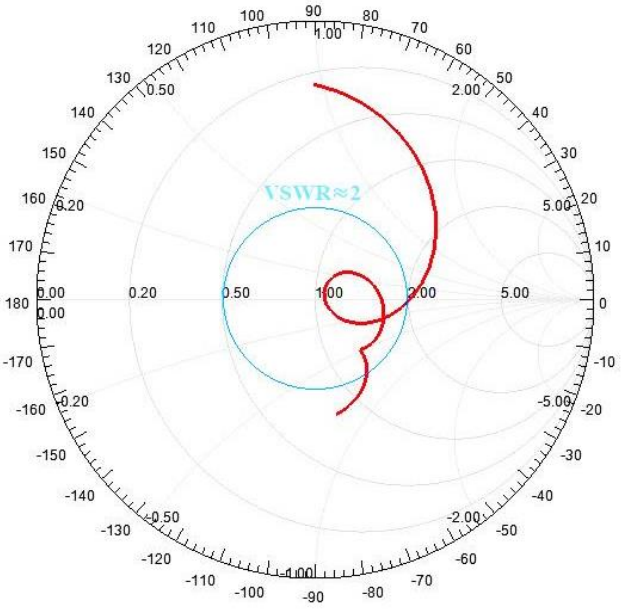

Fig. 9 Smith chart for the proposed antenna

3.2. Radiation Pattern

Figure 10 and Figure 11 show simulated radiation patterns in the E-plane and H-plane at the center frequency of the bands n258 and n257, respectively. The proposed antenna showed promising results in terms of radiation pattern with a maximum total gain of 6.9 dB.

3.3. Mitigation of Fabrication Defects

As shown in Figure 3 and Table 1, all the different parts of the proposed antenna are of equiangular quadrilaterals with mostly integer physical dimensions, drastically decreasing the chances of fabrication errors. Compared to this, the process of physically soldering the parts on the ground plane contains room for inaccuracy. Because the location of the shorting plate in the proposed antenna is selected at the edge of the ground plane, it completely avoids the issue of fabrication inaccuracy. So the spacing between the enhancement plates is the only parameter having the possibility of deviation. If the value of S_e came out to be 3 mm instead of 2.1 mm after the fabrication, it substantially deteriorates the antenna's performance.

Figure 12 shows its effect on the reflection coefficient curve. The impedance bandwidth gets reduced from 11.63 GHz (23.47-35.10 GHz) to 3.49 GHz (23.61-27.10 GHz). A novel resolving technique of providing a symmetric physical inclination (θ_i) to the enhancement plates is presented in Figure 13. In the case of the S_e having the value 3mm, the inclination of 15° to both enhancement plates with respect to the ground plane (towards the co-axial feed) can achieve the impedance bandwidth back to 10.35 GHz (23.33-33.68 GHz) covering both n257 and n258 band once again with a very good matching at the resonance frequency of 25 GHz as shown in Figure 12. The appropriate inclination angle is discovered with the help of an iterative approach. Figure 14 shows the return loss vs frequency graph containing attainable periodic deviated values of S_e with an interval of 0.5 mm starting from 3 mm with its respective θ_i value. Table 2 contains these different values of S_e, θ_i, and the resultant frequency range of operation. By observing Figure 14 and Table 2, it can be observed that the maximum value of the allowable deviation for S_e is 4.5 mm because at S_e equal to 5 mm, the operating range breaks into two bands having very poor matching.

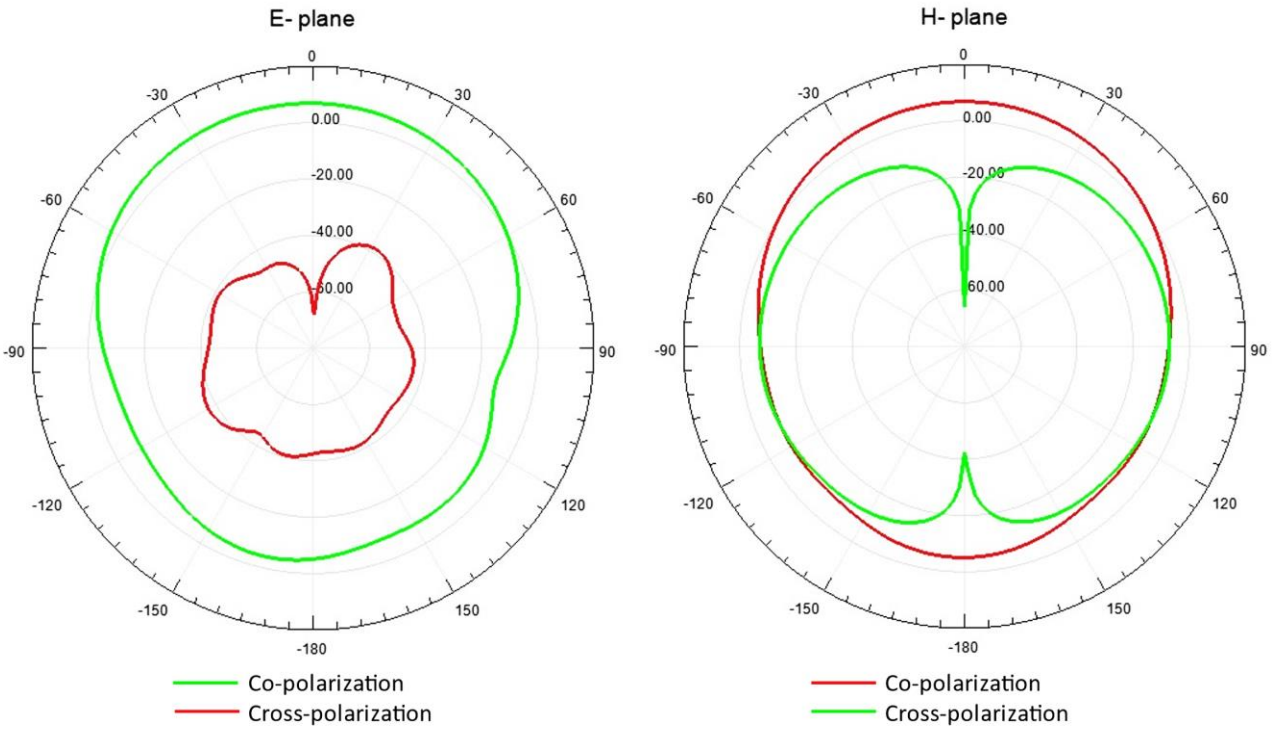

Fig. 10 Simulated radiation patterns in E-plane and H-plane at the frequency of 25.88 GHz

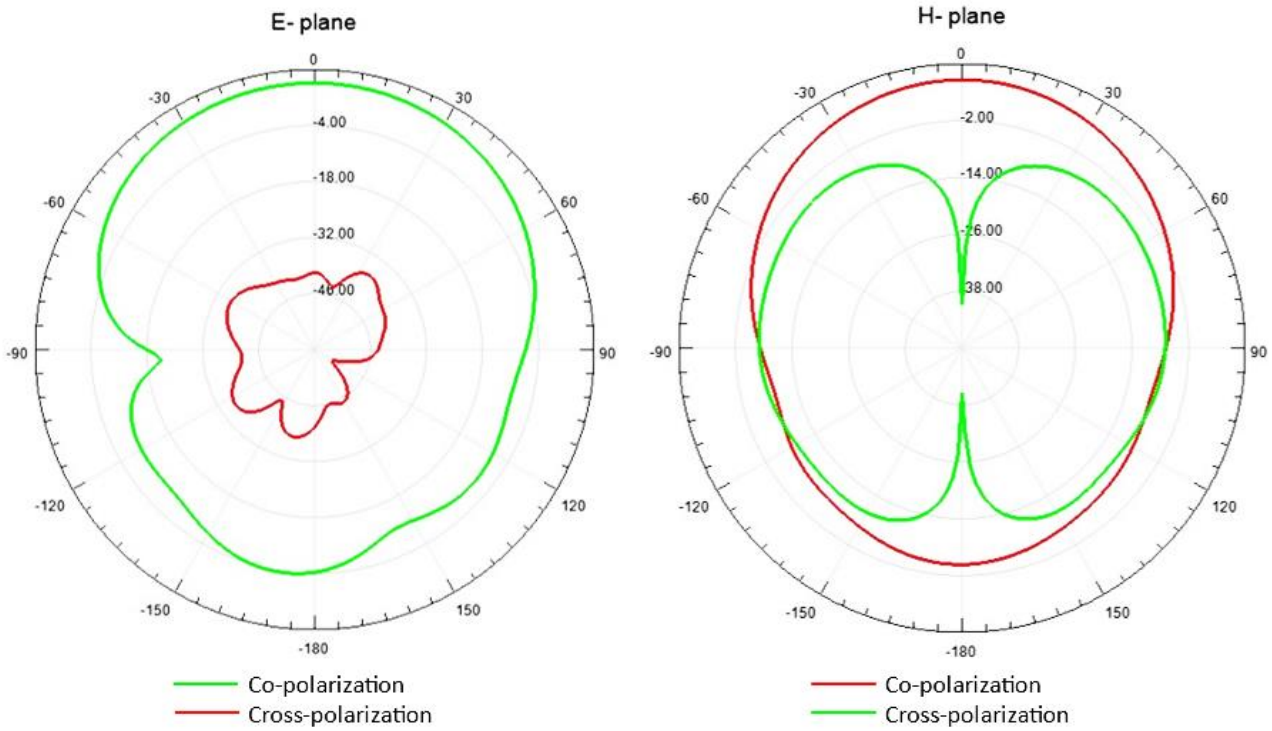

Fig. 11 Simulated radiation patterns in E-plane and H-plane at the frequency of 28 GHz

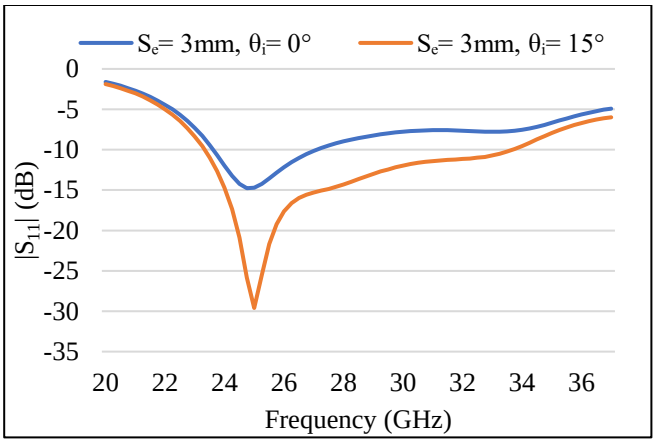

Fig. 12 Reflection coefficient curves for S_e = 3 mm, θ_i = 0° and S_e = 3 mm, θ_i = 15°

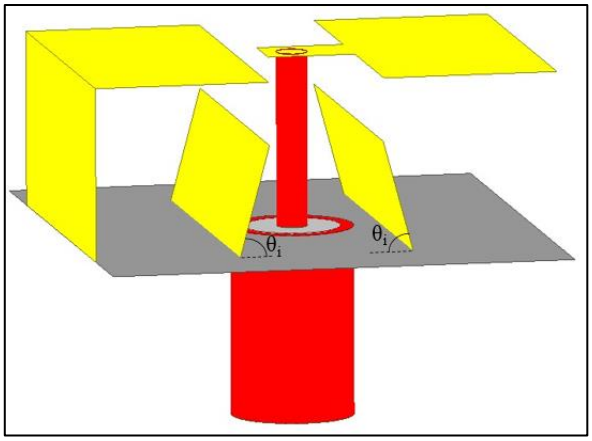

Fig. 13 Proposed magneto-electric dipole geometry for the mitigation of enhancement plate spacing errors

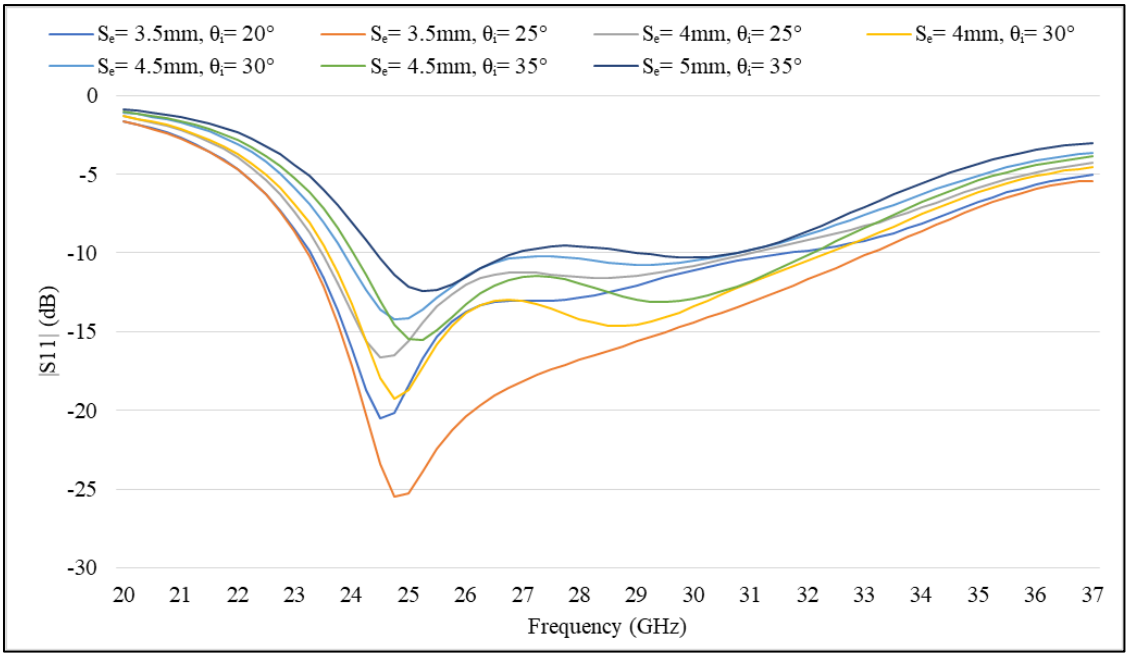

Fig. 14 Return loss vs frequency plots for different values of Se and θi

Table 2. Operating frequency ranges for different combinations of S_e and θ_i

Sr. No.	S_e value	θ_i value	Frequency range of operation (-10dB)
1	3.5 mm	20°	23.31-31.63 GHz
2	3.5 mm	25°	23.29-33.15 GHz
3	4 mm	25°	23.43-30.92 GHz
4	4 mm	30°	23.46-32.31 GHz
5	4.5 mm	30°	23.83-30.75 GHz
6	4.5 mm	35°	24.09-32.11 GHz
7	5 mm	35°	24.41-26.87 GHz & 29.03-30.78 GHz

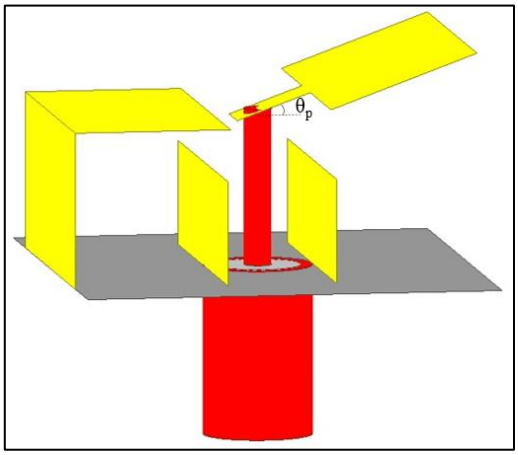

Fig. 15 Proposed magneto-electric dipole geometry for the mitigation of patch angular positioning errors

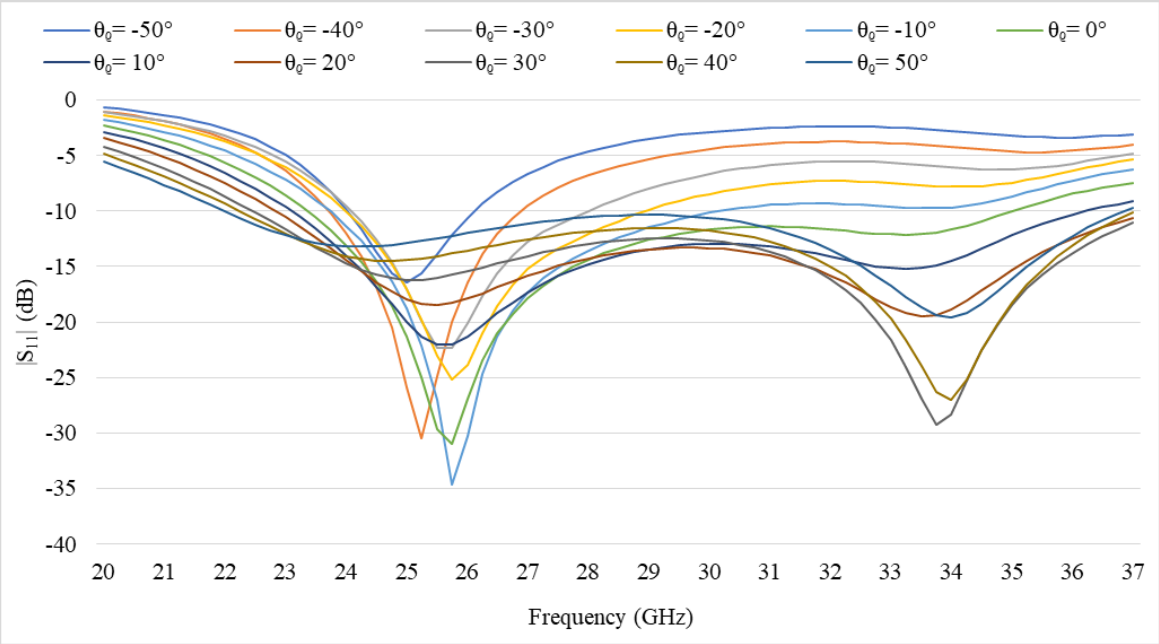

Fig. 16 Parametric analysis for different angular positions of patch

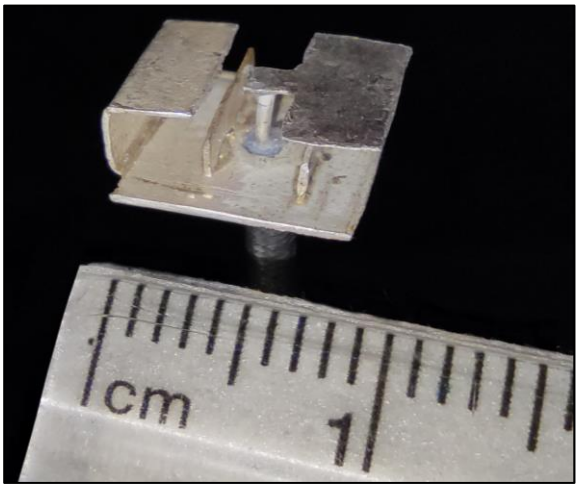

Fig. 17 Fabricated proposed antenna

The other attribute that can be observed is that for the same value of the S_e, as the θ_i increases, the matching increases, and in turn, the higher end of the operating range further extends toward higher frequency. The other possible error after fabrication is patch angular positioning error, as shown in Figure 15. The parametric analysis is performed to find the allowable range for the patch angular position (θ_p), as shown in Figure 16. It can be observed that for the negative value of θ_p, the reflection coefficient shows poor matching. As the value of θ_p decreases below 0°, the matching deteriorates. For the positive angular value, an additional resonance occurs at 34 GHz, and the resonance becomes more and more prominent as the value of θ_p increases (positively). So the allowable range for patch angular position is 0° to 50°.

4. Fabricated Proposed Antenna

As shown in Figure 17, the proposed antenna is volumetrically shaped, due to which silver is used for its manufacturing, considering its malleability and thermal conductivity compared to copper.[24] The proposed antenna uses the soldering technique for fabrication; the higher thermal conductivity of silver makes the process of heat dissipation fast, reducing the possibility of material damage due to overheating while manufacturing. A formstable co-axial cable (SUCOFORM_86) is used to feed the proposed antenna. The center conductor diameter, outer conductor diameter, dielectric constant, and cut-off frequency of the cable are 0.53 mm, 2.1 mm, 2.1 (Polytetrafluoroethylene), and 40 GHz, respectively. Milling machines or 3D printers can be used to increase fabrication accuracy even more.[25,26]

5. Conclusion

The proposed Magneto-electric dipole design has an operating band of 23.47-35.10 GHz, covering both n257 and n258. The novel mitigation technique for the fabrication defects like enhancement plate spacing inaccuracy and patch angular positioning error could be extremely useful considering the volumetric design of the proposed antenna. The major applications of the proposed antenna design can be as unit elements for 5G antenna arrays for the base station. The proposed antenna can also be integrated into smart home devices, industrial IoT devices and autonomous vehicles.

Conflicts of Interest

The authors declare that there is no conflict of interest regarding the publication of this paper.

References

[1] Godfrey Anuga Akpakwu et al., "A Survey on 5G Networks for the Internet of Things: Communication Technologies and Challenges," *IEEE Access*, vol. 6, pp. 3619-3647, 2018. [CrossRef]

[2] Maria Rita Palattella et al., "Internet of Things in the 5G Era: Enablers, Architecture, and Business Models," *IEEE Journal on Selected Areas in Communications*, vol. 34, no. 3, pp. 510-527, 2016. [CrossRef]

[3] Li Da Xu, Wu He, and Shancang Li, "Internet of Things in Industries: A Survey," *IEEE Transactions on Industrial Informatics*, vol. 10, no. 4, pp. 2233-2243, 2014. [CrossRef]

[4] *Measuring Digital Development: Fact and Figures 2021*, ITU publications, vol. 2021, pp. 1-2, 2021.

[5] Jeffrey G. Andrews et al., "What Will 5G Be?," *IEEE Journal on Selected Areas in Communications*, vol. 32, no. 6, pp. 1065-1082, 2014.

[6] Gupta, R. K. Jha, "A Survey of 5G Network: Architecture and Emerging Technologies," *IEEE Access*, vol. 3, pp. 1206-1232, 2014. [CrossRef]

[7] Kumaresh Sheelavant, and R. Sumathi, Charan K V, "Optimal Routing and Scheduling for Cognitive Radio Sensor Networks Using Ensemble Multi Probabilistic Optimization and Truncated Energy Flow Classification Model," *International Journal of Engineering Trends and Technology*, vol. 69, no. 9, pp. 168-178, 2021. [CrossRef]

[8] Theodore S. Rappaport et al., "Millimeter Wave Mobile Communications for 5G Cellular: It Will Work!" *IEEE Access*, vol. 1, pp. 335-349, 2013. [CrossRef]

[9] Zhouyue Pi, and Farooq Khan "An Introduction to Millimeter-Wave Mobile Broadband Systems," *IEEE Communications Magazine*, vol. 49, no. 6, pp. 101-107, 2011. [CrossRef]

[10] Faizan Qamar et al., "Investigation of Future 5G-Iot Millimeter-Wave Network Performance at 38 Ghz for Urban Microcell Outdoor Environment," *Electronics*, vol. 8, no. 5, p. 495, 2019. [CrossRef]

[11] M. Idrees Magray et al., "Co-Design of Conformal 4G LTE and Mmwave 5G Antennas for Smartphones," *2019 IEEE International Symposium on Antennas and Propagation and USNC-URSI Radio Science Meeting*, pp. 701-702, 2019. [CrossRef]

[12] Deepika Sipal et al., "Wideband Millimeter Wave Antenna for 5G Applications with Out-of-Band Rejection," *2020 IEEE Asia-Pacific Microwave Conference (APMC)*, pp. 454-456, 2020. [CrossRef]

[13] Michael Joseph Shundi et al., "Improvements in Spectrum Sharing Towards 5G Heterogeneous Networks," *SSRG International Journal of Electronics and Communication Engineering*, vol. 6, no. 3, pp. 1-9, 2019. [CrossRef]

[14] Yin Chen Chang et al., "A Novel Dual-Polarized Wideband and Miniaturized Low Profile Magneto-Electric Dipole Antenna Array for Mmwave 5G Applications," *IEEE Open Journal of Antennas and Propagation*, vol. 2, pp. 326-334, 2021.

[15] Zhi Ning Chen et al., *Handbook of Antenna Technologies*, 1st Edition Singapore: Springer Singapore, pp. 1971-1972, 2016

[16] Kwai-Man Luk et al., "The Magnetoelectric Dipole—A Wideband Antenna for Base Stations in Mobile Communications," *Proceedings of the IEEE*, vol. 100, no. 7, pp. 2297-2307, 2012. [CrossRef]

[17] Hernan X. Cordova J., "Energy-Efficiency (EE) Performance for 5G Wireless Systems under the Presence of Hardware Impairments," *SSRG International Journal of Electronics and Communication Engineering*, vol. 6, no. 8, pp. 31-37, 2019. [CrossRef]

[18] Kai He et al., "A Wideband Dual-Band Magneto-Electric Dipole Antenna with Improved Feeding Structure," *IEEE Antennas and Wireless Propagation Letters*, vol. 13, pp. 1729-1732, 2014.

[19] Lei Ge, and Kwai Man Luk, "A Low-Profile Magneto-Electric Dipole Antenna," *IEEE Transactions on Antennas and Propagation*, vol. 60, no. 4, pp. 1684-1689, 2012. [CrossRef]

[20] M. D. Huang et al., "Causes of Discrepancies Between Measurements and EM-Simulations of Millimeter-Wave Antennas," *IEEE Antennas and Propagation Magazine*, vol. 55, no. 6, pp. 139-149, 2013. [CrossRef]

[21] D.H. Schaubert et al., "Effect of Microstrip Antenna Substrate Thickness and Permittivity: Comparison of Theories with Experiment," *IEEE Transactions on Antennas and Propagation*, vol. 37, no. 6, pp. 677-682, 1989. [CrossRef]

[22] D. Pozar, and S. Voda, "A Rigorous Analysis of a Microstripline Fed Patch Antenna," *IEEE Transactions on Antennas and Propagation*, vol. 35, no. 12, pp. 1343-1350, 1987. [CrossRef]

[23] Shruti. R. Danve, Manoj S. Nagmode, and Shankar B. Deosarkar, "Transmit Antenna Selection in Massive MIMO: An Energy-Efficient Approach," *International Journal of Engineering Trends and Technology*, vol. 70, no. 12, pp. 170-178, 2022. [CrossRef]

[24] D. R. Smith, and F. R. Fickett, "Low-Temperature Properties of Silver," *Journal of Research of the National Institute of Standard and Technology*, vol. 100, no. 2, pp. 119-171, 1995. [CrossRef]

[25] Roberto Vincenti Gatti, Riccardo Rossi, and Marco Dionigi, "Single-Layer Line-Fed Broadband Microstrip Patch Antenna on Thin Substrates," *Electronics*, vol. 10, no. 1, p. 37, 2020. [CrossRef]

[26] Fanqi Sun et al., "Millimeter-Wave Magneto-Electric Dipole Antenna Array with a Self-Supporting Geometry for Time-Saving Metallic 3-D Printing," *IEEE Transactions on Antennas and Propagation*, vol. 68, no. 12, pp. 7822-7832, 2020. [CrossRef]

[27] Rahul Khadase et al., "In Vitro Testing of Implantable Antenna For Glucose Sensing," *International Journal of Engineering Trends and Technology*, vol. 69, no. 7, pp. 109-113, 2021. [CrossRef]

[28] Oluseun Oyeleke Wikiman et al., "PIFA Antenna Design for Mmwave Body Centric 5G Communication Applications," *SSRG International Journal of Electronics and Communication Engineering*, vol. 6, no. 4, pp. 6-10, 2019. [CrossRef]

[29] Giuseppe Scalise et al., "Magneto-Electric Dipole Antenna for 5-G Applications," *2020 14th European Conference on Antennas and Propagation (EuCAP)*, pp. 1-3, 2020. [CrossRef]

[30] K. -M. Luk, and H. Wong, "A New Wideband Unidirectional Antenna Element," *International Journal of Microwave and Optical Technology*, vol. 1, no. 1, pp. 35-44, 2006.

[31] Ved Prakash, and Krishna Kumar, "Study of PIFA Antenna With Shorting Pin and Plate," *Journal of Emerging Technologies and Innovative Research*, vol. 5, no. 6, pp. 731-736, 2018.

[32] Ravilla Dilli, "Analysis of 5G Wireless Systems in FR1and FR2 Frequency Bands," *2nd International Conference on Innovative Mechanisms for Industry Applications (ICIMIA)*, pp. 767-772, 2020. [CrossRef]